Chemical Engineering Journal 158 (2010) 633–640

Contents lists available at ScienceDirect

Chemical Engineering Journal

journal homepage: www.elsevier.com/locate/cej

Biopolymer-induced microstructure-controlled fabrication of Ni–Al layered double hydroxide films

Hui Wang, Chen Zheng, Feng Li*

State Key Laboratory of Chemical Resource Engineering, Beijing University of Chemical Technology, P.O. BOX 98, Beijing, 100029, PR China

ARTICLE INFO

Article history:
Received 26 October 2009
Received in revised form 29 January 2010
Accepted 4 February 2010

Keywords:
Layered double hydroxide
Film
Sodium alginate
Nanosheet
Carbon nanofibers

ABSTRACT

Novel three-dimensional nanostructured Ni–Al layered double hydroxide (NiAl-LDH) films on sulfonated silicon substrates have been successfully fabricated using a facile biopolymer-induced approach. The structure and morphology of materials were investigated by scanning electron microscopy (SEM), powder X-ray diffraction (XRD), chemical analysis, X-ray photoelectron spectrum (XPS) and high-resolution transmission electron microscopy (HRTEM). The results revealed that unique self-organized NiAl-LDH architectures composed of numerous individual curved nanosheets on substrates could be tuned readily by varying the concentration of initial metal ions with the assistance of sodium alginate. A possible formation mechanism for NiAl-LDH film is proposed, on the basis of the interactions between sodium alginate molecules and NiAl-LDH crystals and between NiAl-LDH crystals and sulfonated substrate. Furthermore, as-formed NiAl-LDH film showed good catalytic activity for the growth of uniform carbon nanofibers with the width of about 200 nm by catalytic chemical vapor deposition of acetylene. The findings in this work are meaningful in understanding the fabrication process of architectures of layered materials on plane substrates and may provide a feasible approach for the control of the microstructure of other functional LDH films.

1. Introduction

Layered double hydroxides (LDHs), known as synthetic anionic clays, are a class of brucite $Mg(OH)_2$-like layered inorganic materials by stacking layers along c-axis [1–3]. LDHs have the general formula $[M_{1-x}^{2+}M_x^{3+}(OH)_2]^{x+}(A^{n-})_{x/n}{\bullet}mH_2O$, where the M^{2+} (Mg^{2+}, Ni^{2+}, Co^{2+}, Cu^{2+} or Zn^{2+}) and M^{3+} (Al^{3+}, Fe^{3+}, Cr^{3+} or Ga^{3+}) cations are divalent and trivalent metal ions coordinated octahedrally by hydroxyl groups to form infinite two-dimensional layers by edge-sharing, and the A^{n-} anion is located between the layers to form stacked layer by electrostatic interactions with positively charged layers. Owing to the characteristic of tunable compositions and exchangeable anions, LDH materials have been widely used as catalysts, catalyst supports, stabilizers in polymer composites, drug delivery materials, adsorbents for wastewater treatment, molecular precursors for chemically tailored functional materials and matrix materials in hybrid composites, etc. [4–9].

Currently, considerable efforts have been devoted to the microstructure-controlled fabrication of LDH films or coatings built on different substrates at low temperatures from aqueous solution for the purpose of developing various novel applications. Some fabrication methods for organizing primary building units into special three-dimensional hierarchical nanostructures of LDH particles on plane substrates have been reported mostly by colloidal assembly technique using colloidal nanocrystals [10–14] or delaminated nanosheets of LDHs as building blocks or by in situ crystallization technique involving direct growth of LDH crystallites [15–19]. For example, O'Hare and coworkers have investigated the growth of oriented hybrid cobalt-based LDH films on organically functionalized Au and Si substrates [20]. More importantly, these nanostructured LDH films are found to have potential applications as monolithic catalysts [18], corrosion-resistant materials [19], biosensors [21] and modified electrode materials [22].

On the other hand, since the morphological diversity of inorganic materials has a significant impact on functional diversification and potential applications, control of the unusual morphology and size of nanomaterials is stimulating worldwide interests in areas of materials science [23–28]. In particular, biomolecule-assisted approach has been found to exhibit a more promising and tremendous potentials for controllably organizing small lower dimensional primary species into various complicated three-dimensional ordered nanostructures [29–33], as a result of the fact that biomolecules including polypeptides, proteins and viruses have special structures and attracting self-assembling functions for novel nanomaterials as structure-directing agents.

* Corresponding author. Tel.: +86 10 64451226; fax: +86 10 64425385.
E-mail address: lifeng_70@163.com (F. Li).

1385-8947/$ – see front matter © 2010 Elsevier B.V. All rights reserved.
doi:10.1016/j.cej.2010.02.007

Table 1
The synthesis parameters for LDH films.

Samples	Sulfonation time for Si substrate (h)	Dosage of sodium alginate (g)	Total concentration of initial metal ions (M)
LDH-a	72	1.2	0.075
LDH-b	120	1.2	0.075
LDH-c	120	0	0.075
LDH-d	120	1.2	0.045
LDH-e	120	1.2	0.30

Considering that the nucleation and growth processes for the formation of inorganic films have significant effects on their microstructure and morphology, it remains a big challenge to develop more effective and facile protocols for the control of microstructure of individual LDH crystallites on certain substrates for practical use in devices in current LDH research. Up to now, there has been no report of the direct growth of LDH films on inorganically modified silicon substrates with the assistance of organic template. In this contribution, we established a low-temperature and environmentally benign surfactant-free approach to fabricate three-dimensional nanostructured NiAl-LDH films on sulfonated silicon substrate in the presence of water-soluble biopolymer (sodium alginate). The results indicate that sodium alginate may act as organic template to induce the formation of special curved NiAl-LDH nanosheets on substrate. Moreover, it is found that the quite uniform carbon nanofibers (CNFs) could be achieved by catalytic chemical vapor deposition (CCVD) of acetylene over as-formed NiAl-LDH film.

2. Experimental section

2.1. Sulfonation of Si substrate

A piece of silicon wafer was first cleaned ultrasonically by acetone and ethanol for eliminating any greasy track and then abundantly rinsed with distilled water. The surface of clean silicon substrates was sulfonated by dipping in 98% sulfuric acid for 72 or 120 h at room temperature. It is then ultrasonically washed with deionized water, and dried under N_2 gas flow.

2.2. Fabrication of LDH films

All chemicals were supplied by Beijing Chemicals Co. Ltd., and were used as received. In a typical synthesis, urea, $Ni(NO_3)_2$ and $Al(NO_3)_3$ with the Ni^{2+}/Al^{3+} molar ratio of 2.0 and the molar ratio of urea to metal cations of 2.7 were dissolved in 80 mL of deionized water to present a clear solution with the total concentrations of metal cations of 0.075 M. Sequentially, 1.2 g of sodium alginate was added into the solution. Then, 10 mm × 20 mm sulfonated Si substrate was immersed into above solution for 2 h. The resulting solution was transferred to 100 mL of Teflon-lined autoclave and treated at the temperature of 80 °C for 48 h. The as-formed NiAl-LDH film and NiAl-LDH precipitate collected from solution were washed with deionized water for four times, and then dried at 70 °C for 12 h in air. For comparison, we also synthesized NiAl-LDH film without the introduction of sodium alginate. The synthesis parameters of all NiAl-LDH film samples are listed in Table 1.

2.3. Growth of CNFs

CNFs were prepared in a quartz tube inside a horizontal tube furnace equipped with mass controller and temperature-programmed control by CCVD of acetylene. After loading NiAl-LDH films in an alumina boat, the furnace was firstly raised to 500 °C with 5 °C/min under nitrogen gas flow (flow rate: 60 standard-state $cm^3\ min^{-1}$ (sccm)). When reaching 500 °C, H_2 gas (6 sccm) was introduced and the temperature was maintained for 40 min. Subsequently, H_2 gas was switched off and the furnace was further heated to 700 °C, and C_2H_2 gas was switched on with a flow rate of 6 sccm. The temperature was maintained at 700 °C for 60 min. After the reaction, N_2 gas was continued till the furnace was cooled to room temperature.

2.4. Characterization

X-ray photoelectron spectra (XPS) of samples were recorded on a Thermo VG ESCALAB250 X-ray photoelectron spectrometer at a pressure of about 2×10^{-9} Pa using Mg Kα radiation at 1253.6 eV as the excitation source. The binding energy (BE) calibration of the spectra has been referred to carbon 1s peak, located at BE = 284.8 eV.

Powder X-ray diffraction (XRD) patterns of samples were collected using a Shimadzu XRD-6000 diffractometer under the following conditions: 40 kV, 30 mA, graphite-filtered Cu Kα radiation (λ = 0.15418 nm). The samples were step-scanned in steps of 0.04° (2θ) using a count time of 10 s/step.

Elemental analysis for metal ions in samples was performed using a Shimadzu ICPS-75000 inductively coupled plasma emission spectrometer (ICP-ES). Solutions were prepared by dissolving the samples in dilute hydrochloric acid (1:1).

Scanning electron microscopy (SEM) microanalyses of samples were made using a Hitachi S4700 apparatus with the applied voltage of 20 kV.

High-resolution transmission electron microscopy (HRTEM) was taken on a JEM-3010 transmission electron microscope. The sample for this characterization was prepared by dipping carbon coated copper TEM grids with dilute ethanol suspensions of the sample powder.

3. Results and discussion

3.1. Fabrication and morphology of NiAl-LDH films

It has been reported by Lei and coworkers that the oriented MgAl-LDH films were formed on sulfonated polystyrene substrates [15]. In our case, silicon substrates were sulfonated with concentrated sulfuric acid in order to produce ionized surfaces for immobilization of NiAl-LDH crystallites. The surface chemical states of sulfonated substrates obtained are analyzed by XPS within a range of binding energy (BE) of 0–1200 eV (Fig. 1). Core levels of Si 2p, S 2p and O 1s can be identified, and no other contaminant species are detectable. The fine spectrum of the S 2p peak present in the inset shows a BE value of 168.7 eV, corresponding to the bonding of sulfur in sulfonate groups. The results prove that sulfonate groups were grafted onto silicon substrate. Moreover, the extent of sulfonation of silicon substrate (i.e. the surface coverage of sulfonate groups) increases with reaction time, as determined by the values of S/Si ratio measured by XPS (0.23 for 72 h and 0.30 for 120 h, respectively).

The phase purity of NiAl-LDH obtained in the presence of sodium alginate using the total concentration of metal ions of 0.075 M was determined by XRD. As shown in Fig. 2a, the XRD pattern of as-deposited NiAl-LDH powder scraped from substrate of LDH-b film presents the characteristic reflections of hydrotalcite-like materials with a series of wide symmetric (0 0 *l*) peaks at low 2θ angles corresponding to the basal spacing around 7.8 Å and high order diffractions [2], indicative of carbonate as charge compensating anions in the interlayer. No other crystalline phases are detected. The wide reflection peaks indicate the nature of small crystallite size. Consequently, the coherent diffraction domain size (thickness of sheet) of NiAl-LDH crystallites in the *c* direction (the stacking direction, perpendicular to the layers), which is estimated by means of the Scherrer equation [34], is about 4.2 nm. Additionally,

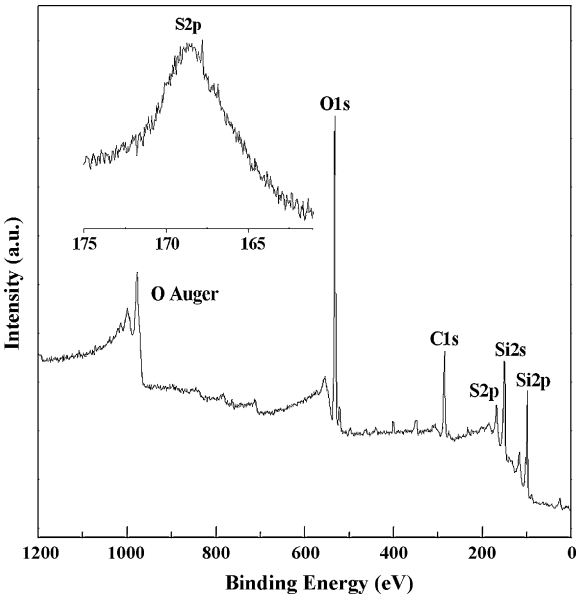

Fig. 1. Representative XPS survey of sulfonated Si substrate (inset: S 2p spectrum).

NiAl-LDH precipitate collected from aqueous solution under the identical experimental conditions also exhibits the characteristic reflections of LDH phase (Fig. 2b). In comparison with those of NiAl-LDH powder scraped, the (0 0 *l*) peak intensities of NiAl-LDH precipitate are enhanced in spite of little change of the full width of (0 0 *l*) peaks, suggesting that the crystallinity of LDH precipitate is higher but the thickness of LDH crystallites is still identical to that of LDH crystallites grown on substrate.

SEM images of NiAl-LDH films obtained in the presence of sodium alginate are shown in Fig. 3a–d. It is seen that a small amount of particulate or disorder platelet-like precipitate of LDH-a film is dispersed on substrate with low surface coverage of sulfonate groups (Fig. 3a and b), while NiAl-LDH layer of LDH-b film presents a regular three-dimensional architecture on substrate with high surface coverage of sulfonate groups (Fig. 3c and d). The result indicates that the formation of high-quality LDH film

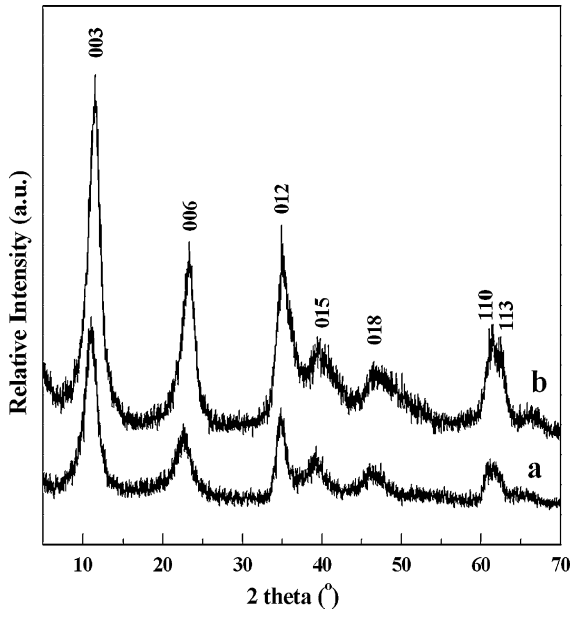

Fig. 2. XRD patterns of NiAl-LDH scraped from LDH-b film (a) and NiAl-LDH precipitate collected from aqueous solution (b).

is dependent on the sulfonation level for silicon substrate. Closer observation from high-magnification SEM image (Fig. 3d) shows that such architecture of LDH-b film is built by unusual curved and intercrossed nanosheets. The thickness of nanosheets is observed to be approximately 5–10 nm, consistent with the above XRD result. The kind of novel NiAl-LDH architecture has not been reported before. In comparison with LDH films reported in the literature [15], the sheets of LDH crystallites in LDH-b film are much thinner and the feature of curved nanosheets is more remarkable. It suggests the existence of templating effect of sodium alginate on the formation of LDH crystallites. Also, it can be clearly seen from Fig. 3e that the morphology of LDH-c film prepared by conventional method without sodium alginate is quite different from that of LDH-b film. The high-magnification image reveals that NiAl-LDH layer only exhibits a compact arrangement of nanoparticles with roughly spherical shape (Fig. 3f). The formation of LDH-c film in the absence of sodium alginate should involve transportation of metal cations to the sulfonated substrate surface, adsorption and enrichment of the cations on the substrate, followed by the nucleation and growth of LDH crystals. The above results confirm that the introduction of sodium alginate can play the role of inducing the formation of curved nanosheets of LDH crystals, in spite of instinct hardness and rigidity of tightly stacking LDH layers [2,35]. The reasons are explored in detail in the following sections.

To further investigate the microstructure of LDH-b film, NiAl-LDH nanosheets scraped from substrate were characterized by HRTEM. The typical image of an individual nanosheet (Fig. 4a) indicates clearly the sheet-like feature of NiAl-LDH crystallites, which agrees with the broad reflection peaks in XRD pattern. HRTEM image in Fig. 4b indicates the presence of an interplanar distance of about 0.24 nm that is characteristic of (0 1 2) plane, further confirming the formation of well-crystallized LDH phase. On the other hand, interestingly, as shown in Fig. 5a, LDH precipitate formed in aqueous solution presents a marigold-like spherical superstructure with the average diameter of about 1.0 μm, where all nanosheets formed almost keep nearly perpendicular to the spheres and become compact and uniform. High-magnification SEM image in Fig. 5b illustrates that these microspheres consist of a large number of intercrossed and curved or contorted nanosheets with the thickness of ~10 nm, which are similar to those building blocks of three-dimensional LDH architecture in LDH-b film. It is well known that owing to their anisotropic structure consisting of a hexagonal planar layer arrangement of octahedral oxygen-coordinated metal ions [2], LDH materials usually tend to exhibit the morphological characteristics of hexagonal platelets, in which the a and b dimensions (parallel to the layers) are much larger than the c dimension (perpendicular to the layers). Thanks to this intrinsic feature of crystal structure, marigold-like spherical superstructure of LDH particles formed in aqueous solution, like other unique ordered superstructures of belt-like, flower-like, hollow shell shaped ones and so forth reported in the literature [36–41], could be synthesized by self-assembly approach of metastable building blocks of LDH nanosheets under experimental conditions.

The aforementioned XRD, SEM and HRTEM results verify conclusively that NiAl-LDH layer on substrate and NiAl-LDH precipitate formed in solution have same interior microstructure and phase of LDH crystallites. Furthermore, elemental analysis by ICP-ES gives the Ni/Al atomic ratio of about 2.1 for LDH-b film and LDH precipitate in aqueous solution, which is consistent with that in the initial synthesis mixture. It indicates that there is no preferential enrichment of Al^{3+} over Ni^{2+} on substrate surface in spite of its higher charge density. As a result, the LDH nanosheets in LDH film are closely related to the nanosheets constructing marigold-like LDH microspheres in aqueous solution.

Total concentrations of initial metal ions were further varied in order to investigate the growth process of nanostructured

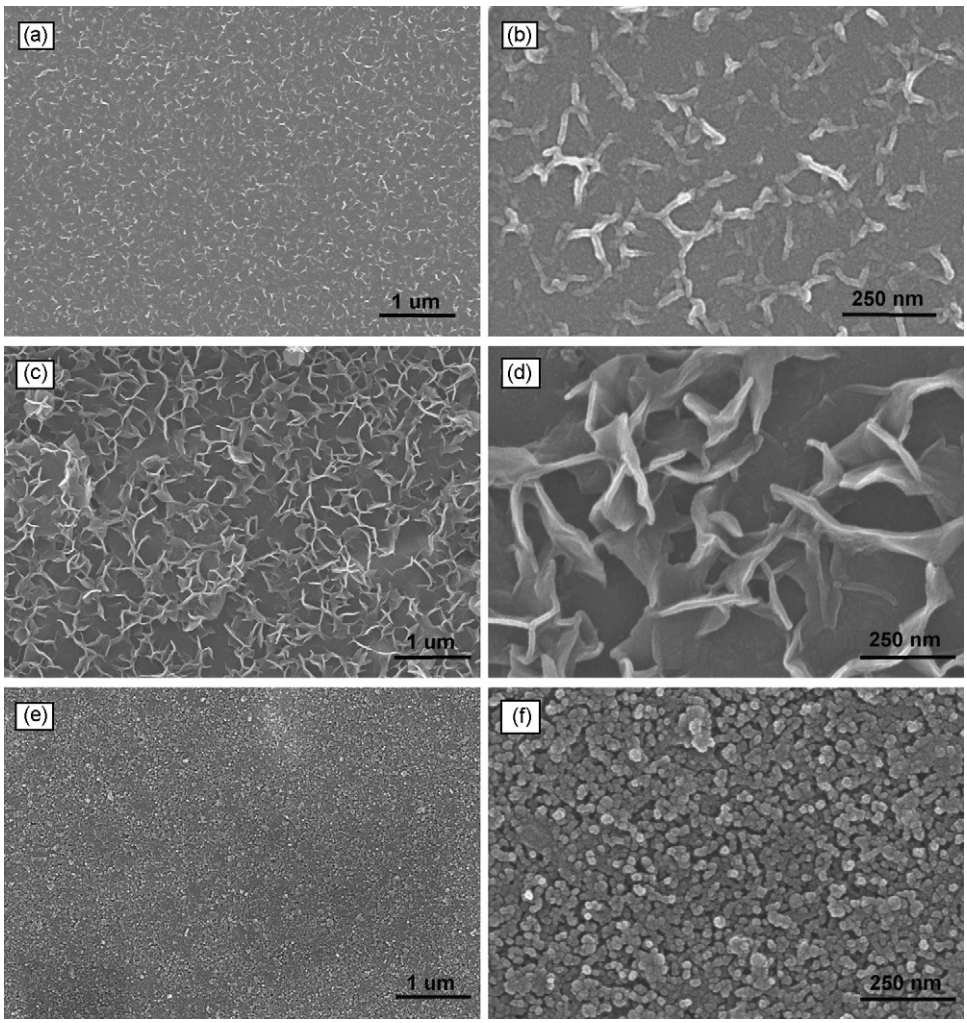

Fig. 3. SEM images of LDH-a film (a and b), LDH-b (c and d) and LDH-c film (e and f).

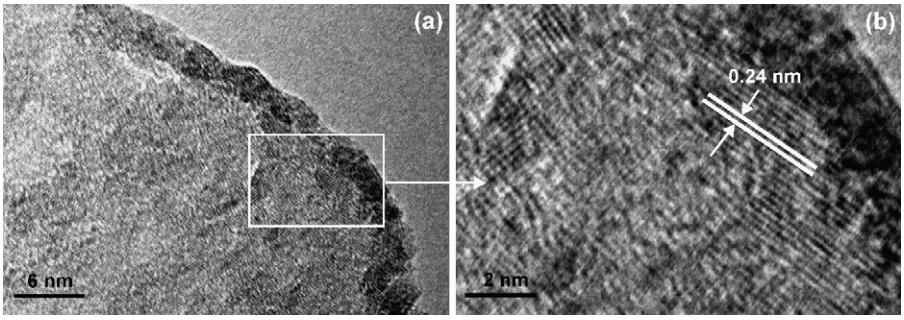

Fig. 4. HRTEM images of individual nanosheet of LDH-b film.

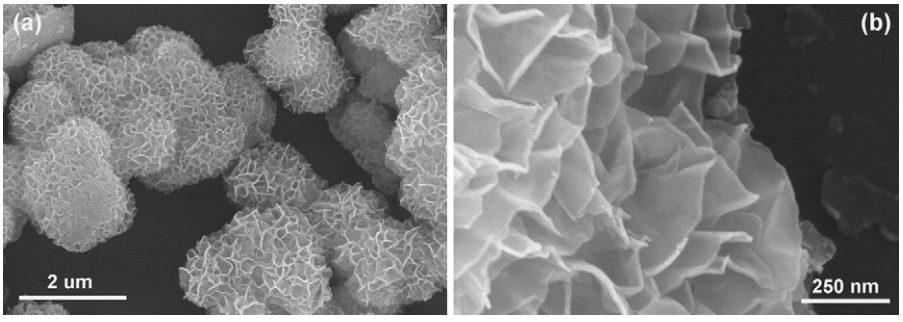

Fig. 5. SEM images of NiAl-LDH precipitate collected from aqueous solution.

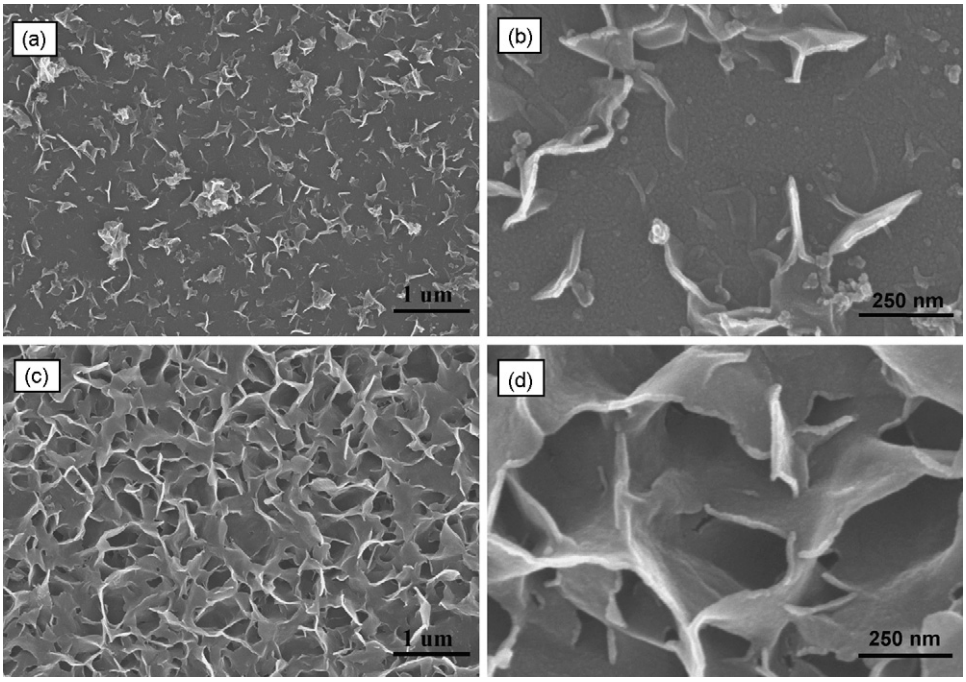

Fig. 6. SEM images of NiAl-LDH films obtained in the presence of sodium alginate using different total concentrations of initial metal ions. (a and b) 0.045 M and (c and d) 0.3 M.

NiAl-LDH films. It is apparently observed from Fig. 6a that if the total concentration of metal ions was reduced to 0.045 M but keeping other reaction conditions constant, a small quantity of sheet-like NiAl-LDH particles are dispersed on substrate. As shown in Fig. 6b, although some curved NiAl-LDH nanosheets connects with each other in LDH-d film, the distance between them is relatively wider, that is, the distribution of NiAl-LDH nanostructure is sparser, compared to those in the case of total concentration of metal ions of 0.075 M. When the total concentration of metal ions is further increased to 0.3 M, one can find from Fig. 6c that well-defined architecture of NiAl-LDH particles in LDH-e film formed is composed of a larger number of more densely packed intercrossed and curved nanosheets. Note from Fig. 6d that formed nanosheets with the thickness of about 10–15 nm connect closely together and get larger. The reason is that increasing the total concentration of metal ions might make more metal ions interact with sodium alginate molecules, which can significantly promote the growth of NiAl-LDH crystals on substrate. With the total concentration of metal ions, however, the increase in stacking thickness of nanosheets cannot be obviously observed. In addition, with the increasing concentration of metal ions, NiAl-LDH aggregates collected from solution also presents more densely packed marigold-like morphology of microspheres, which well agrees with the change of NiAl-LDH architecture on substrate. The results elucidate that increasing total concentration of initial metal ions leads to both little change in the thickness of nanosheets and the progressive increase in the lateral dimension of nanosheets, suggesting that the crystal growth of NiAl-LDH on substrate is preferential along *a* direction. As a result, it can be concluded that the total concentration of metal ions has a crucial influence on the growth of NiAl-LDH nanosheets, and high total concentration of metal ions facilitates the formation of more densely packed three-dimensional architectures.

3.2. The formation mechanism for LDH films

It is well known that sodium alginate is a naturally derived linear anionic copolymer originated from 1,4-linked β-D-mannuronic acid (M-block) and α-L-guluronic acid (G-block) residues [42,43]. There are a large number of negatively charged carboxyl groups within its skeletal framework, which are hydrophilic groups and can provide coordination sites with chelating cations when it is plunged into aqueous solution. Therefore, sodium alginate may act as a kind of organic biomineralization template to induce the formation of special morphologies for inorganic materials.

In the present synthesis system, Ni^{2+} and Al^{3+} ions in aqueous solution can form coordination complexes with carboxyl groups of sodium alginate through the electrostatic attraction. At the temperatures of 80 °C, urea, a very weak Brønsted base ($pK_b = 13.8$) [44], will hydrolyze slowly and give NH_4^+, CO_2 and OH^- [45], thus raising the pH value of aqueous reaction solution. Consequently, Ni^{2+} and Al^{3+} ions can coprecipitate homogeneously and form NiAl-LDH crystal nuclei in bulk solution. Sequentially, the nuclei grow into small crystals. Meanwhile, sodium alginate molecules dissolved in water form regular self-assembled organic superstructure with the flexural or tortuous chains, and are inclined to attach on the (1 1 0) lattice surface due to the fact that LDH crystals most commonly grow faster in (1 1 0) plane than in (0 0 3) plane [46], which inhibits the stacking of LDH nanocrystals into larger platelets in three-dimensional orientation. Moreover, it can be supposed that the quite thin sheet-like layers of LDH crystals can be deformed by applying a bending force originating from coordination sites of sodium alginate molecules with metal ions at the curved inorganic–organic interfaces, which weakens the bonding interaction on the atomic scale [47], thus leading to the formation of the curved nanosheets.

In bulk solution, primary NiAl-LDH nanosheets freely form aggregate and self-assemble into ordered three-dimensional superstructure in order to minimize their surface energy. On the contrary, when the strong electrostatic interaction between the positively changed lattices of NiAl-LDH nuclei and the negatively charged sulfonated substrate surface becomes favorable, these nuclei attaching to sodium alginate molecules are energetically adsorbed on substrate surface, and thus the subsequent growth of NiAl-LDH crystals is restricted on substrate. Finally, the random orientation of curved NiAl-LDH nanosheets formed at the phase boundary further constructs three-dimensional nanostructured

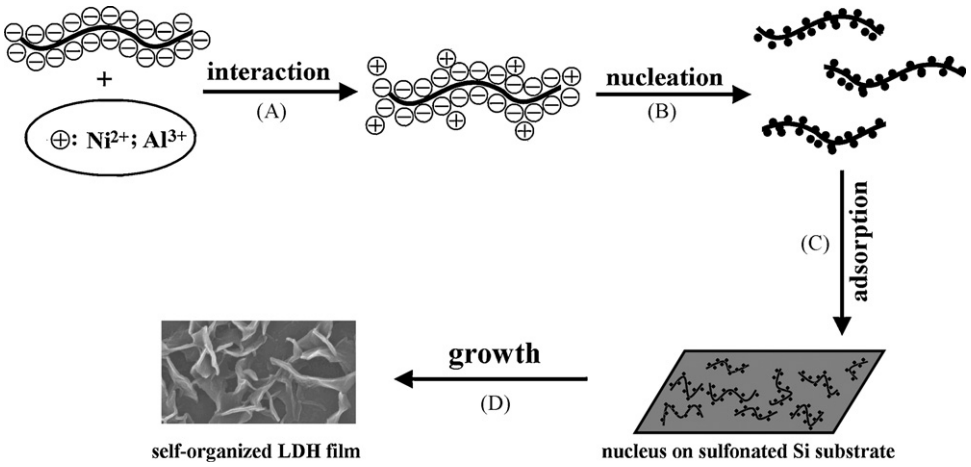

Fig. 7. Schematic illustration of the possible formation mechanism for three-dimensional nanostructured NiAl-LDH film. (A) Electrostatic attraction between metal ions and carboxylic groups of sodium alginate; (B) Sodium alginate-induced nucleation of LDH crystals; (C) Adsorption of LDH crystals on sulfonated substrate surface; (D) Growth of LDH nanosheets.

films. However, the anchored sulfonate groups could be resolved from the surface of Si substrate after the reaction due to high pH value of solution and long reaction time, evidenced by the fact that no S species is detectable from XPS analysis of LDH-b film. In general, the formation of NiAl-LDH architecture proceeds by the nucleation in bulk solution, the surface adsorption of nuclei on substrate and oriented growth of LDH crystals. Fig. 7 illustrates schematically the possible formation mechanism of three-dimensional nanostructured NiAl-LDH film with the assistance of sodium alginate.

3.3. The growth of CNFs

Fig. 8 shows the SEM images for as-synthesized carbon materials over LDH-b and LDH-c films. It is clearly seen that the use of LDH-c film results in the formation of twisting CNFs with nonuniform diameters and coarse surface (Fig. 8a and b). In contrast, it is observed that a large number of uniform CNFs with the identical width of about 200 nm distributed in random orientation in a wide field over the LDH-b film (Fig. 8c), and the length of the fibers reaches to several tens micrometers. Additionally, dark/light contrasts are clearly observed along the axial direction of fibers. The light contrast at the top of the carbon fibers corresponds to large catalyst particles with the uniform size identical to the width of fibers, suggesting a top growth mechanism of CNFs. A close observation reveals that each individual fiber is uniform with the average width of 200 nm, and that in most cases there is another slim zigzag-like fiber with the width of about 40 nm attaching on the surface of main CNFs (Fig. 8d). This type of carbon nanostructure is, however, less observed or reported in previous studies and may have potential applications in the fields of catalysis, adsorption and other areas.

It is well known that during high temperature CCVD of carbonaceous gas, transition metals (iron, nickel, cobalt and their alloys) supported over materials with high surface area can be used as active catalysts for the growth of CNFs [48–51]. As for LDH

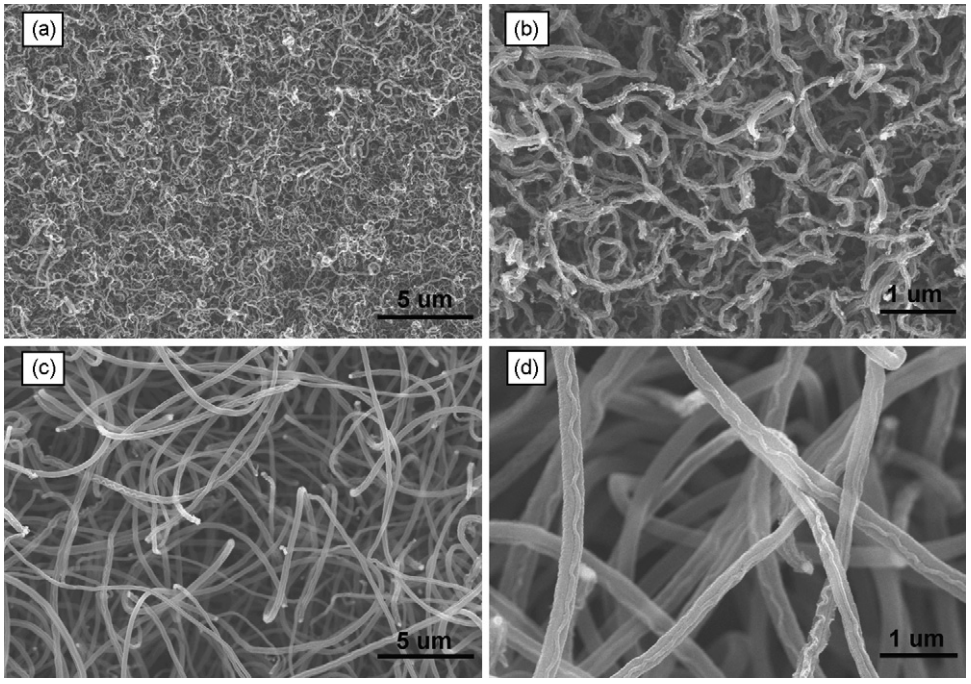

Fig. 8. SEM images of CNFs obtained over LDH-c film (a and b) and LDH-b film (c and d).

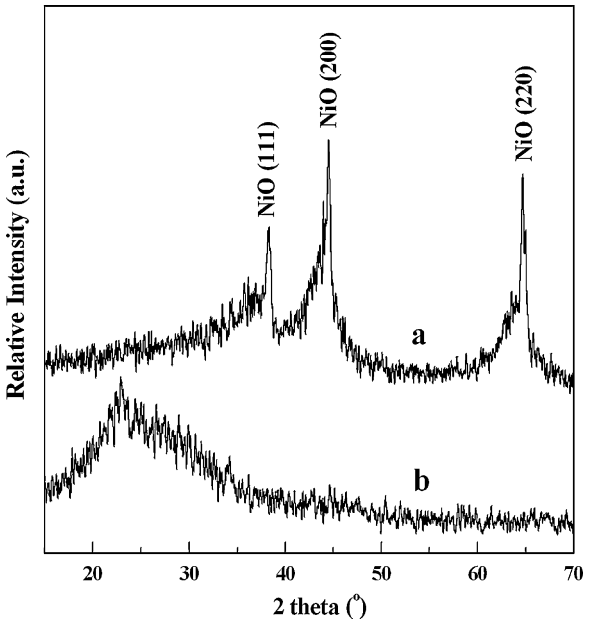

Fig. 9. XRD patterns of calcined NiAl-LDH powder scraped from LDH-b film at 500 °C prior to the reduction (a) and carbon products (b).

materials, metallic cobalt and nickel particles can be obtained by reducing calcined NiAl-LDH precursors on the basis of the homogenous ordered prearrangement of catalytically active component in LDH at an atomic level [52–54]. In order to further understand the mechanism of synthesis of CNFs, XRD analysis for calcined LDH-b film at 500 °C collected from the tube furnace prior to the reduction was carried out. It is found that the XRD pattern only demonstrates the characteristic (1 1 1), (2 0 0) and (2 2 0) reflections of cubic NiO phase (JCPDS 47–1049) (Fig. 9a). Additionally, the broad reflections reveal the presence of some amorphous products, e.g., alumina or $NiAl_2O_4$ spinel [55]. The result suggests that after calcination of LDH-b film, Ni species in the form of NiO phase can highly disperse on oxide matrix, probably favoring the formation of highly dispersed active metal particles during the treatment with H_2 and C_2H_2 gases. In addition, a broadened peak in the range between 20° and 30° are observed in XRD pattern of carbon products over LDH-b film (Fig. 9b) and no characteristic reflections of meal and graphitic carbon appear, confirming the feature of amorphous CNFs and highly dispersed metal catalyst particles. As a result, in the present case, the three-dimensional architecture of NiAl-LDH film composed of disperse and individual nanosheets may facilitate the dispersion and stabilization of active metal particles over metal oxide matrix, and thus the diffusion of acetylene to resulting catalyst surface should be able to favor the growth of uniform high-quality CNFs.

4. Conclusions

In this work, we developed a new synthetic route to special three-dimensional nanostructured NiAl-LDH films on sulfonated silicon substrate by a facile biopolymer-assisted approach. The results indicate that sodium alginate can be used as structure-directing agent for the formation of unusual curved NiAl-LDH nanosheets. Furthermore, the morphology of NiAl-LDH architectures on substrate can be diversified by using different total concentrations of initial metal ions. A possible formation mechanism for nanostructured NiAl-LDH films is proposed. Furthermore, it is found that uniform CNFs could be successfully obtained by CCVD of acetylene over as-formed LDH films and showed good catalytic activity. The present findings prove that it is viable to synthesize unique three-dimensional LDH architectures via a biopolymer-directed crystal growth and mediated process, which promotes the development of self-organization of inorganic building blocks on plane substrate. It is expected that this promising and feasible approach can be applied to the control of the microstructure of other functional LDH films.

Acknowledgments

We gratefully thank the financial support from the National Natural Science Foundation of China, 973 Program (2009CB939802), 111 Project (No. B07004) and Changjiang Scholars and Innovative Research Team in Universities (IRT 0406).

References

[1] G.R. Williams, D. O'Hare, Towards understanding, control and application of layered double hydroxide chemistry, J. Mater. Chem. 16 (2006) 3065–3074.
[2] D.G. Evans, R.C.T. Slade, Structural aspects of layered double hydroxides, Struct. Bond. 119 (2006) 1–87.
[3] J. He, M. Wei, B. Li, Y. Kang, D.G. Evans, X. Duan, Preparation of layered double hydroxides, Struct. Bond. 119 (2006) 89–119.
[4] F. Li, X. Duan, Applications of layered double hydroxides, Struct. Bond. 119 (2006) 193–223.
[5] X. Liu, M. Wei, D.G. Evans, X. Duan, Structured chiral adsorbent formed by cyclodextrin modified layered solid film, Chem. Eng. Sci. 64 (2009) 2226–2233.
[6] L. Zou, X. Xiang, J. Fan, F. Li, Single-source precursor to complex metal oxide monoliths with tunable microstructures and properties: the case of Mg-containing materials, Chem. Mater. 19 (2007) 6518–6527.
[7] Z. Gu, A.C. Thomas, Z.P. Xu, J.H. Campbell, G.Q. Lu, In vitro sustained release of LMWH from MgAl-layered double hydroxide nanohybrids, Chem. Mater. 20 (2008) 3715–3722.
[8] F. Leroux, C. Taviot-Guého, Fine tuning between organic and inorganic host structure: new trends in layered double hydroxide hybrid assemblies, J. Mater. Chem. 15 (2005) 3628–3642.
[9] L. Desigaux, M.B. Belkacem, P. Richard, J. Cellier, P. Léone, L. Cario, F. Leroux, C. Taviot-Guého, B. Pitard, Self-assembly and characterization of layered double hydroxide/DNA hybrids, Nano Lett. 6 (2006) 199–204.
[10] J.H. Lee, S.W. Rhee, D.Y. Jung, Orientation-controlled assembly and solvothermal ion-exchange of layered double hydroxide nanocrystals, Chem. Commun. (2003) 2740–2741.
[11] J.H. Lee, S.W. Rhee, D.Y. Jung, Solvothermal ion exchange of aliphatic dicarboxylates into the gallery space of layered double hydroxides immobilized on Si substrates, Chem. Mater. 16 (2004) 3774–3779.
[12] J.H. Lee, S.W. Rhee, D.Y. Jung, Selective layer reaction of layer-by-layer assembled layered double hydroxide nanocrystals, J. Am. Chem. Soc. 129 (2007) 3522–3523.
[13] Z. Liu, R. Ma, M. Osada, N. Iyi, Y. Ebina, K. Takada, T. Sasaki, Synthesis, anion exchange, and delamination of Co–Al layered double hydroxide: assembly of the exfoliated nanosheet/polyanion composite films and magneto-optical studies, J. Am. Chem. Soc. 128 (2006) 4872–4880.
[14] L.Y. Wang, C. Li, M. Liu, D.G. Evans, X. Duan, Large continuous, transparent and oriented self-supporting films of layered double hydroxides with tunable chemical composition, Chem. Commun. (2007) 123–125.
[15] X.D. Lei, L. Yang, F.Z. Zhang, D.G. Evans, X. Duan, Synthesis of oriented layered double hydroxide thin films on sulfonated polystyrene substrates, Chem. Lett. 34 (2005) 1610–1611.
[16] H.Y. Chen, F.Z. Zhang, S.S. Fu, X. Duan, In situ microstructure control of oriented layered double hydroxide monolayer films with curved hexagonal crystals as superhydrophobic materials, Adv. Mater. 18 (2006) 3089–3093.
[17] Y.F. Gao, M. Nagai, Y. Masuda, F. Sato, W.S. Seo, K. Koumoto, Surface precipitation of highly porous hydrotalcite-like film on Al from a zinc aqueous solution, Langmuir 22 (2006) 3521–3527.
[18] Z. Lu, F.Z. Zhang, X.D. Lei, L. Yang, S.L. Xu, X. Duan, In situ growth of layered double hydroxide films on anodic aluminum oxide/aluminum and its catalytic feature in aldol condensation of acetone, Chem. Eng. Sci. 63 (2008) 4055–4062.
[19] F.Z. Zhang, L.L. Zhao, H.Y. Chen, S.L. Xu, D.G. Evans, X. Duan, Corrosion resistance of superhydrophobic layered double hydroxide films on aluminum, Angew. Chem. Int. Ed. 47 (2008) 2466–2469.
[20] J.H. Lee, Y. Du, D. O'Hare, Growth of oriented thin films of intercalated α-cobalt hydroxide on functionalized Au and Si substrates, Chem. Mater. 21 (2009) 963–968.
[21] D. Shan, C. Mousty, S. Cosnier, Subnanomolar cyanide detection at polyphenol oxidase/clay biosensors, Anal. Chem. 76 (2004) 178–183.
[22] J.X. He, K. Kobayashi, Y.M. Chen, G. Villemure, A. Yamagishi, Electrocatalytic response of GMP on an ITO electrode modified with a hybrid film of Ni(II)–Al(III) layered double hydroxide and amphiphilic Ru(II) cyanide complex, Electrochem. Commun. 3 (2001) 473–477.
[23] J.S. Son, X.D. Wen, J. Joo, J. Chae, S. Baek, K. Park, J.H. Kim, K. An, J.H. Yu, S.G. Kwon, S.H. Choi, Z. Wang, Y.W. Kim, Y. Kuk, R. Hoffmann, T. Hyeon, Large-scale soft

colloidal template synthesis of 1.4 nm thick CdSe nanosheets, Angew. Chem. Int. Ed. 48 (2009) 6861–6864.
[24] C. Chen, W. Chen, J. Lu, D. Chu, Z. Huo, Q. Peng, Y. Li, Transition-metal phosphate colloidal spheres, Angew. Chem. Int. Ed. 48 (2009) 4816–4819.
[25] D. Portehault, C. Sophie, N. Nassif, E. Baudrin, J.P. Jolivet, A core-corona hierarchical manganese oxide and its formation by an aqueous soft chemistry mechanism, Angew. Chem. Int. Ed. 47 (2008) 6441–6444.
[26] D. Walsh, S. Mann, Fabrication of hollow porous shells of calcium carbonate from self-organizing media, Nature 377 (1995) 320–323.
[27] B. Liu, H.C. Zeng, Fabrication of ZnO "Dandelions" via a modified Kirkendall process, J. Am. Chem. Soc. 126 (2004) 16744–16746.
[28] L. Qi, H. Cölfen, M. Antonietti, Crystal design of barium sulfate using double-hydrophilic block copolymers, Angew. Chem. Int. Ed. 39 (2000) 604–607.
[29] P. Liang, Q. Shen, Y. Zhao, Y. Zhou, H. Wei, I. Lieberwirth, Y. Huang, D. Wang, D. Xu, Petunia-shaped superstructures of $CaCO_3$ aggregates modulated by modified chitosan, Langmuir 20 (2004) 10444–10448.
[30] Q. Wu, H. Cao, Q. Luan, J. Zhang, Z. Wang, J.H. Warner, A.A.R. Watt, Biomolecule-assisted synthesis of water-soluble silver nanoparticles and their biomedical applications, Inorg. Chem. 47 (2008) 5882–5888.
[31] T. Douglas, E. Strable, D. Willits, A. Aitouchen, M. Libera, M. Young, Protein engineering of a viral cage for constrained nanomaterials synthesis, Adv. Mater. 14 (2002) 415–418.
[32] L.Y. Chen, Z.D. Zhang, Biomolecule-assisted synthesis of $In(OH)_3$ hollow spherical nanostructures constructed with well-aligned nanocubes and their conversion into C-In_2O_3, J. Phys. Chem. C 112 (2008) 18798–18803.
[33] M. Knez, A.M. Bittner, F. Boes, C. Wege, H. Jeske, E. Maiß, K. Kern, Biotemplate synthesis of 3-nm nickel and cobalt nanowires, Nano Lett. 3 (2003) 1079–1082.
[34] Y. Zhao, F. Li, R. Zhang, D.G. Evans, X. Duan, Preparation of layered double-hydroxide nanomaterials with a uniform crystallite size using a new method involving separate nucleation and aging steps, Chem. Mater. 14 (2002) 4286–4291.
[35] S.A. Solin, D. Hines, S.K. Yun, T.J. Pinnavaia, M.F. Thorpe, Layered rigidity in 2D disordered Ni–Al layer double hydroxides, J. Non-Cryst. Solids 182 (1995) 212–220.
[36] G. Hu, D. O'Hare, Unique layered double hydroxide morphologies using reverse microemulsion synthesis, J. Am. Chem. Soc. 127 (2005) 17808–17813.
[37] B. Li, J. He, Multiple effects of dodecanesulfonate in the crystal growth control and morphosynthesis of layered double hydroxides, J. Phys. Chem. C 112 (2008) 10909–10917.
[38] B. Li, J. He, D.G. Evans, Experimental investigation of sheet flexibility of layered double hydroxides: one-pot morphosynthesis of inorganic intercalates, Chem. Eng. J. 144 (2008) 124–137.
[39] P. Gunawan, R. Xu, Synthesis of unusual coral-like layered double hydroxide microspheres in a nonaqueous polar solvent/surfactant system, J. Mater. Chem. 18 (2008) 2112–2120.
[40] L. Li, R. Ma, N. Iyi, Y. Ebina, K. Takada, T. Sasaki, Hollow nanoshell of layered double hydroxide, Chem. Commun. (2006) 3125–3127.
[41] V. Prevot, N. Caperaa, C. Taviot-Guého, C. Forano, Glycine-assisted hydrothermal synthesis of NiAl-layered double hydroxide nanostructures, Cryst. Growth Des. 9 (2009) 3646–3654.
[42] W. Lu, S. Gao, J. Wang, One-pot synthesis of Ag/ZnO self-assembled 3D hollow microspheres with enhanced photocatalytic performance, J. Phys. Chem. C 112 (2008) 16792–16800.
[43] T.M. Siddaramaiah, Mruthyunjaya Swamy, B. Ramaraj, J.H. Lee, Sodium alginate and its blends with starch: thermal and morphological properties, J. Appl. Polym. Sci. 109 (2008) 4075–4081.
[44] J.M. Oh, S.H. Hwang, J.H. Choy, The effect of synthetic conditions on tailoring the size of hydrotalcite particles, Solid State Ionics 151 (2002) (2002) 285–291.
[45] C. Yan, D. Xue, Self-assembled MgO nanosheet and its precursor, J. Phys. Chem. B 109 (2005) 12358–12361.
[46] Y. Zhao, J. He, Q.Z. Jiao, D.G. Evans, X. Duan, Selectivity of crystal growth direction and control of particle size in layered double hydroxides, Chin. J. Inorg. Chem. 17 (2001) 573–579.
[47] J. He, T. Kunitake, Are ceramic nanofilms a soft matter, Soft Mater. 2 (2006) 119–125.
[48] N.M. Rodriguez, A review of catalytically grown carbon nanofibers, J. Mater. Res. 8 (1993) 3233–3250.
[49] G.B. Zheng, K. Kouda, H. Sano, Y. Uchiyama, Y.F. Shi, H.J. Quan, A model for the structure and growth of carbon nanofibers synthesized by the CVD method using nickel as a catalyst, Carbon 42 (2004) 635–640.
[50] R.T.K. Baker, M.S. Kim, A. Chambers, C. Park, N.M. Rodriguez, The relationship between metal particle morphology and the structural characteristics of carbon deposits, in: C.H. Bartholomew, G.A. Fuentes (Eds.), Catalyst deactivation. Elsevier Science B.V., Amsterdam, Netherlands, 1997, pp. 99–109.
[51] I. Alstrup, A new model explaining carbon-filament growth on nickel, iron, and Ni–Cu alloy catalysts, J. Catal. 109 (1988) 241–251.
[52] H.I. Hima, X. Xiang, L. Zhang, F. Li, Novel carbon nanostructures of caterpillar-like fibers and interwoven spheres with excellent surface superhydrophobicity produced by chemical vapor deposition, J. Mater. Chem. 18 (2008) 1245–1252.
[53] X. Xiang, L. Zhang, H.I. Hima, F. Li, D.G. Evans, Co-based catalysts from Co/Fe/Al layered double hydroxides for preparation of carbon nanotubes, Appl. Clay Sci. 42 (2009) 405–409.
[54] X. Xiang, H.I. Hima, H. Wang, F. Li, Facile synthesis and catalytic properties of nickel-based mixed-metal oxides with mesopore networks from a novel hybrid composite precursor, Chem. Mater. 20 (2008) 1173–1182.
[55] B. Rebours, J.B. d'Espinose de la Caillerie, O. Clause, Decoration of nickel and magnesium oxide crystallites with spinel-type phases, J. Am. Chem. Soc. 116 (1994) 1707–1717.